

Supporting Information

for

Thermal hysteresis induced by external pressure in a 3D Hofmann-type SCO-MOF

Yue Li,^{a*} Qing-Rong Kong,^a Ying Guo,^a Zheng Tang^b

^a*College of Chemistry and Chemical Engineering, Xiamen University, Xiamen 361005, Fujian Province, People's Republic of China. E-mail: liyue1105@sina.cn*

^b*Key Laboratory of Cluster Science of Ministry of Education, School of Chemistry and Chemical Engineering, Liangxiang Campus, Beijing Institute of Technology, Beijing 102488, People's Republic of China.*

Table S1. Crystal structure and refinement details for compounds **1** and **2** at different temperature.

	Compound 1		Compound 2	
Temp (K)	293	95	250	100
formula	FePtC ₁₆ N ₆ O ₄ H ₁₈ Br ₂		FePdC ₁₆ N ₆ O ₄ H ₁₈ Br ₂	
M	769.12		680.43	
cryst syst	tetragonal		tetragonal	
space group	<i>P</i> 4/ <i>m</i>		<i>P</i> 4/ <i>m</i>	
a, Å	7.4386(2)	7.3121(5)	7.4285(7)	7.2533(5)
b, Å	7.4386(2)	7.3121(5)	7.4285(7)	7.2533(5)
c, Å	13.733(2)	13.3878(18)	13.648(3)	13.346(2)
α, deg	90	90	90	90
β, deg	90	90	90	90
γ, deg	90	90	90	90
V, Å ³	759.88(13)	715.80(14)	753.1(2)	702.16(14)
Z	1	1	1	1
D _c , g cm ⁻³	1.681	1.784	1.500	1.609
μ, mm ⁻¹	7.729	8.205	3.757	4.029
F(000)	362.0	362.0	330.0	330.0
goodness-of-fit on F ²	1.201	1.077	1.136	1.112
R1 (I ≥ 2σ(I)) ^a	0.0757	0.0561	0.0672	0.0806
wR2 (all data) ^a	0.1936	0.1554	0.2215	0.2422

a: $I \geq 2\sigma(I)$: $R_1 = \sum |F_o| - |F_c| / \sum |F_o|$, $wR_2 = \{\sum [w(F_o^2 - F_c^2)^2] / \sum [w(F_o^2)^2]\}^{1/2}$.

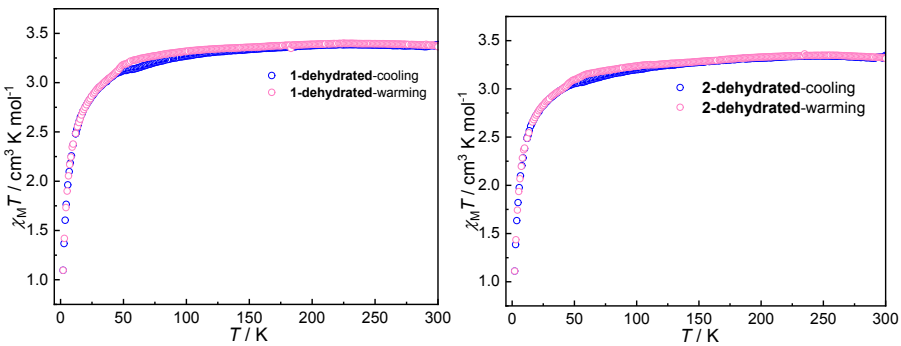


Fig. S1 The $\chi_M T$ versus T plots for compounds **1-dehydrated** and **2-dehydrated**.

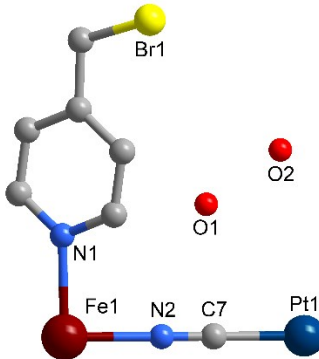


Table S2. The $\text{Fe}^{\text{II}}\text{--N}$ bond distances in compounds **1** and **2** at different temperature.

T / K	Compound 1		Compound 2	
	293	95	250	100
$\text{Fe}^{\text{II}}\text{--N}_{\text{dbdp}} (\text{\AA})$	2.20(2)	2.022(12)	2.129(11)	2.023(14)
$\text{Fe}^{\text{II}}\text{--N}_{\text{NC}} (\text{\AA})$	2.132(12)	2.032(11)	2.132(7)	2.002(9)
$\text{Fe}^{\text{II}}\text{--N}_{\text{ave}} (\text{\AA})$	2.167(6)	2.027(12)	2.130(9)	2.013(12)

Table S3. The $\text{Fe}\cdots\text{Fe}$ distances and Σ_{Fe} of $\{\text{FeN}_6\}$ at different temperature for compounds **1** and **2**.

T / K	Compound 1		Compound 2	
	293	95	250	100
$d_1(\text{Fe}\cdots\text{Fe}) (\text{\AA})$	7.439	7.312	7.428	7.253
$d_2(\text{Fe}\cdots\text{Fe}) (\text{\AA})$	13.733	13.388	13.648	13.346
Σ_{Fe} of $\{\text{FeN}_6\}$ ($^{\circ}$)	12.0	4.8	9.6	6.8

$$\sum_{(i=1)}^{12} |\varphi_i - 90^\circ|$$

Table S4. The host-host, host-guest and guest-guest interactions in compounds **1** and **2**.

	Compound 1		Compound 2	
Temperature	293 K	95 K	250 K	100 K
C1—H1···O1 (Å)	2.62(7)	2.49(13)	2.57(9)	2.44(8)
Br1···Br1 (Å)	3.02(1)	2.75(9)	2.85(3)	2.66(7)
O1···O2 (Å)	2.95(1)	2.86(17)	3.13(2)	2.99(12)

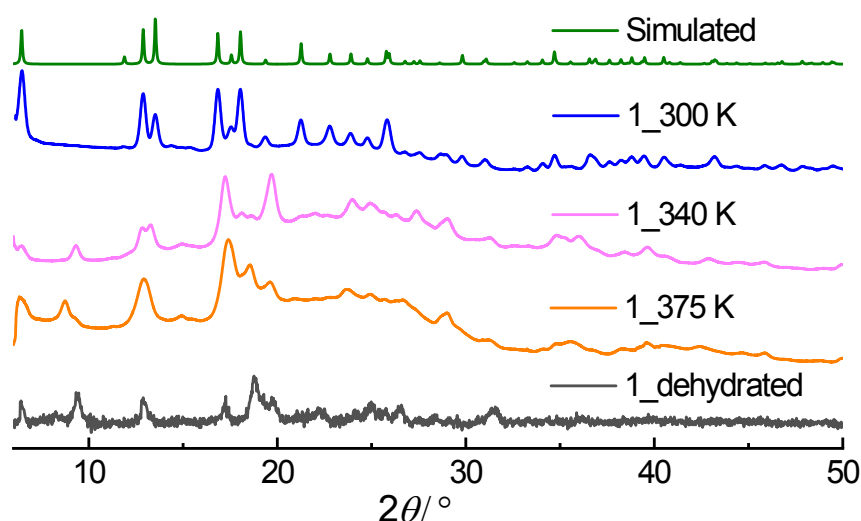


Fig. S3 The PXRD patterns of compound **1** at different temperature.

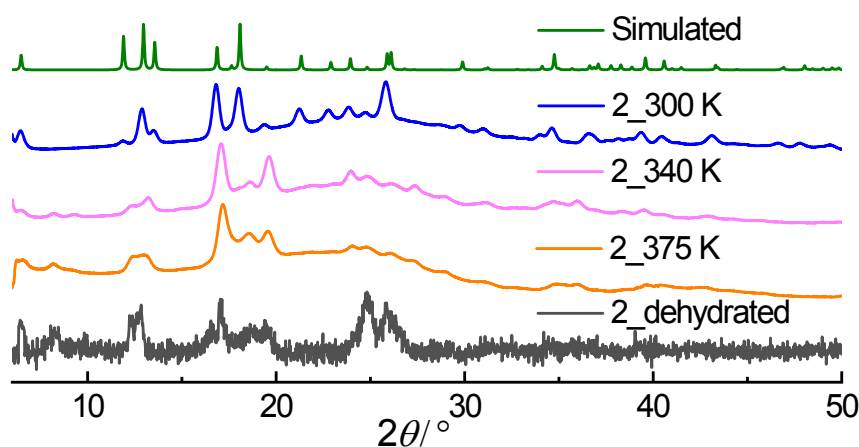


Fig. S4 The PXRD patterns of compound **2** at different temperature.

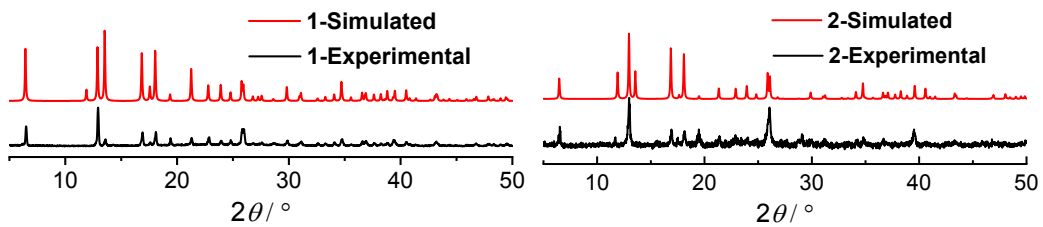


Fig. S5 The PXRD data of compounds **1** and **2** at room temperature collected for each batch.

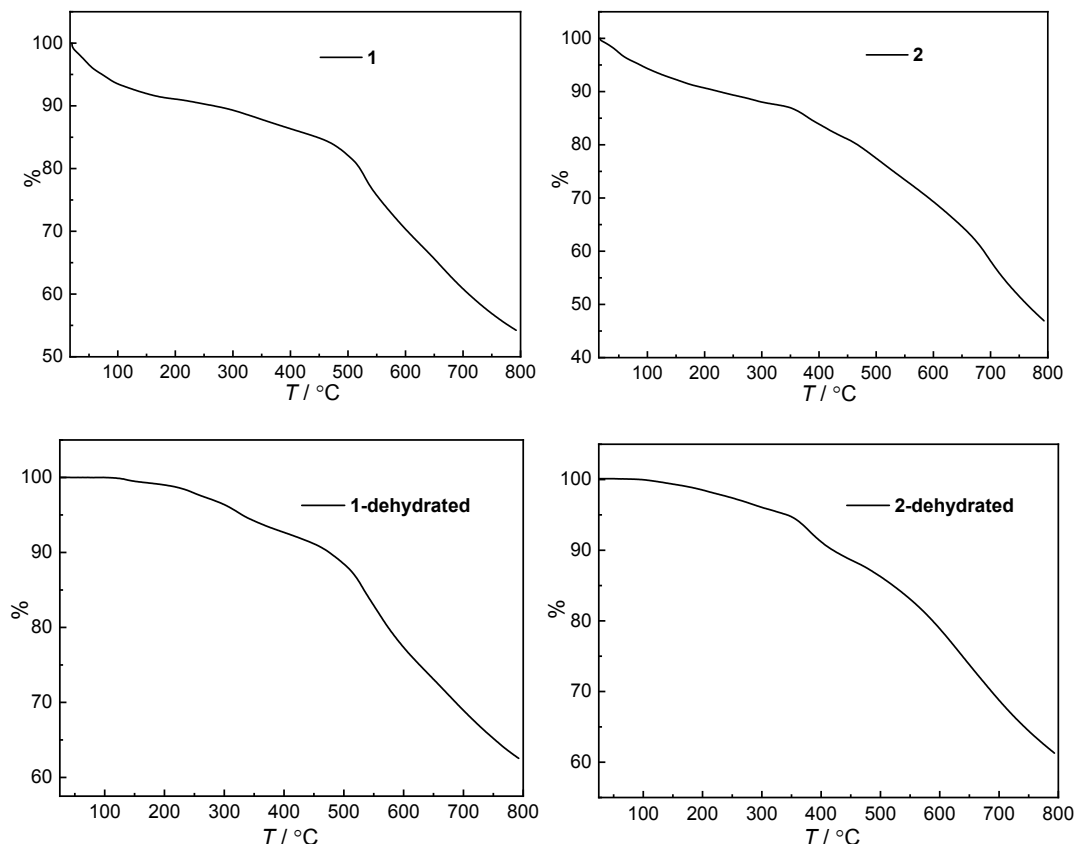


Fig. S6 The TGA plots of compounds **1**, **2** and the dehydrated samples.

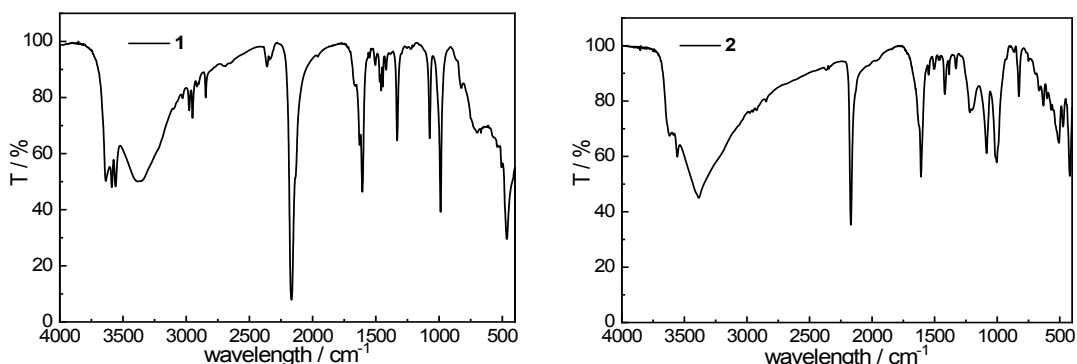


Fig. S7 The FIT-IR plots of compounds **1** and **2**.